Journal of Building Engineering 111 (2025) 113148

Contents lists available at ScienceDirect

Journal of Building Engineering

journal homepage: www.elsevier.com/locate/jobe

Design of steel plate concrete (SC) walls with cross-ties under out-of-plane forces

Jamshaid Sawab [a], Avinash Gautam [a], Peng Liang [b], Jiaji Wang [b,*], Y.L. Mo [a]

[a] Department of Civil and Environmental Engineering, University of Houston, Houston, TX, 77204, USA
[b] Department of Civil Engineering, The University of Hong Kong, Hong Kong, China

ARTICLE INFO

Keywords:
Steel Plate-Concrete (SC)
Out-of-plane loading
Composite Structures
Nuclear Containment Structures
Cross-ties
UHPC
Structural Design

ABSTRACT

This study proposes design guidelines to predict the capacity of Steel Plate – Concrete (SC) walls under out-of-plane forces. It includes a detailed explanation of SC walls behavior and failure mechanisms. An SC wall under out-of-plane forces could reach a desired failure mechanism such as flexure or shear only if the composite action between the steel plate and concrete is sufficient. Otherwise, debonding, the failure mechanism associated with composite action, could govern. A design equation is derived to predict the composite action capacity accurately. The design guidelines and the proposed equation are validated using an experimental database of eight SC beams under varying a/d ratios, longitudinal reinforcement ratio, transverse reinforcement ratio, and concrete strength. A systematic comparison between test results and proposed design guidelines is conducted showing that the proposed method offers high accuracy and safety over existing methods. The findings clarify the interaction between flexural, shear and composite capacities and provide practical design methods for both conventional SC composite walls and steel-Ultra high performance concrete composite walls.

1. Introduction

The Composite Steel Plate Concrete (SC) structural system presents an innovative alternative to the conventional Reinforced Concrete (RC) structural system. It provides numerous advantages including accelerated onsite construction, enhanced material security, reduced construction duration, and improved structural performance. The SC system consists of two steel plates with a layer of concrete sandwiched between them. These steel plates serve as permanent formwork, making the system highly suitable for prefabrication and rapid assembly. In comparison to RC, the SC system exhibits superior strength and ductility, increased stiffness, and considerable energy dissipation capacity. The application of Composite Steel Plate Concrete (SC) structures has seen a rapid increase in recent decades within the field of structural engineering. They are employed in various critical applications such as containment walls for nuclear power plants, tall buildings, and shield tunnels. [1–3]. Steel Plate Concrete (SC) has been extensively utilized in nuclear containment structures, including the AP1000 (Fig. 1) and US-APWR (Advanced Pressurized Water Reactor) to reduce construction time [4].

The advantages of composite structures can be categorized into two main areas: (1) construction and (2) structural performance. Below are the advantages related to construction [5].

* Corresponding author.
E-mail address: cewang@hku.hk (J. Wang).

https://doi.org/10.1016/j.jobe.2025.113148
Received 15 January 2025; Received in revised form 3 June 2025; Accepted 6 June 2025
Available online 13 June 2025

(1) Steel plates reduce construction time/costs by eliminating formwork acquisition, installation, and removal. The comparison of material/labor requirements between RC and SC systems by Takeuchi et al. [6] in ABWR construction is shown in Fig. 2.
(2) Congestion of reinforcement in highly reinforced concrete structures could be avoided by using the Steel Plate Concrete (SC) structural system.
(3) SC modules using steel plates of standard dimensions could minimize waste and reduce construction costs compared to conventional rebar reinforcement, which requires cutting and sizing.
(4) SC elements are typically prefabricated. The modules' assembly is much simpler than built-up steel walls since the welded connections consist of straight segments making it easier to weld on site.
(5) Steel plates can be externally treated and inspected for corrosion. Therefore, the design life of the structure is improved.

The advantages related to structural performance of SC structures include.

(1) SC structures offer enhanced impact and blast resistance, crucial for critical installations such as nuclear containments [7].
(2) SC structures have increased stiffness and strength due to the confinement effect and the higher amount of steel plate reinforcement.
(3) In shear-governed RC walls, rebar placement at 45° aligns with principal stress direction to mitigate pinching effect [8], but is impractical in construction. SC structures inherently orient steel plates along principal stress, eliminating pinching and improving ductility under reversed cyclic loads.

From the mechanics perspective, when integrity is achieved between steel plate and concrete, SC structures can fully utilize the individual strengths of these materials. To facilitate an effective force-transfer mechanism between steel plates and concrete, a variety of techniques are employed, including the use of cross-ties, shear studs, J-hooks, and the preparation of profiled or textured surfaces on steel plates.

Profiled/textured steel surfaces may lead to early interfacial shear failure due to bond slip between concrete and steel plates. Overlapping shear studs can mitigate bond slip progression but do not contribute significantly to out-of-plane shear resistance, thus requiring additional shear resistance measures. Cross-ties (welded to steel plates and embedded in concrete) are highly efficient for SC module construction in terms of time, cost, and quality [9,10], while enhancing shear load capacity. A typical cross-tie configuration is illustrated in Fig. 3.

The SC structural system is increasingly used in nuclear containment walls, where high safety margins lead to thick, heavily reinforced concrete walls prone to rebar congestion, prolonged construction time, and higher costs. SC modules offer economic efficiency and shorter construction periods, making them ideal for small modular reactors (SMRs).

In addition to the general type of generated loading (i.e. dead load, live load, and earthquake load), nuclear containments are subjected to design internal pressure *P*. The different combinations of dead load, live load, internal pressure, and earthquake loading can give rise to in-plane and out-of-plane stresses in the containment wall. The stresses that develop from the applied loading in a nuclear containment structure are illustrated in Fig. 4. A thorough understanding of SC elements under within the plane and outside the plane applied loads are important to develop analysis tools, design guidelines, and recommendations. This study investigates the behavior of SC walls when subjected to out-of-plane forces.

Out-of-plane shear and bending stresses occur at structural discontinuities (e.g., locations A and B in Fig. 4), around openings, and at wall-foundation joints (location A). Stresses at location A can be mitigated by equalizing deformations above/below the

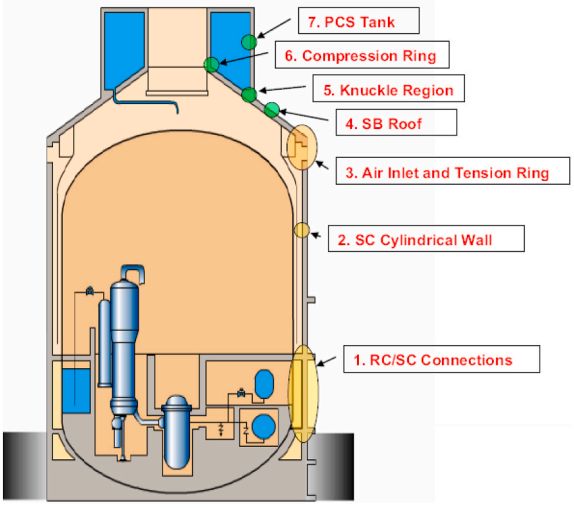

Fig. 1. AP 1000 nuclear power plant [4].

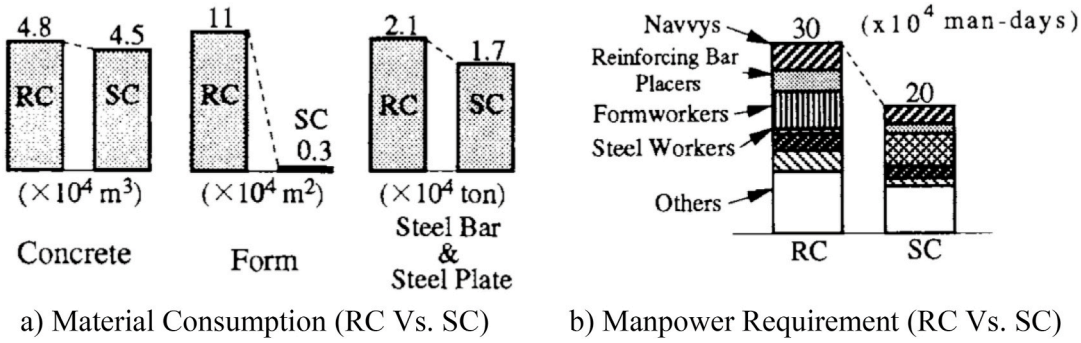

Fig. 2. Feasibility study on an ABWR for Comparing RC with SC structural systems [6].

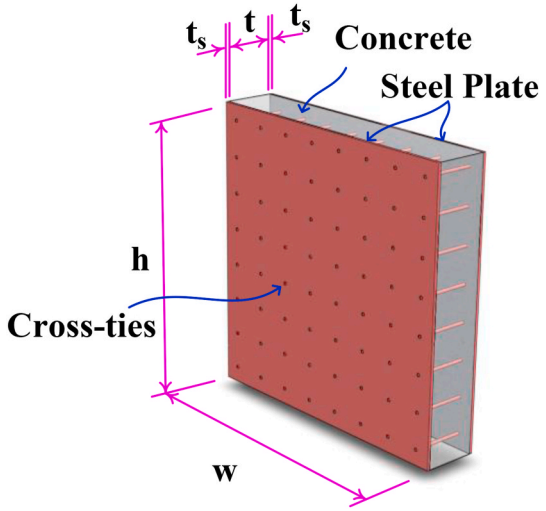

Fig. 3. Steel Plate-Concrete element with tie bars

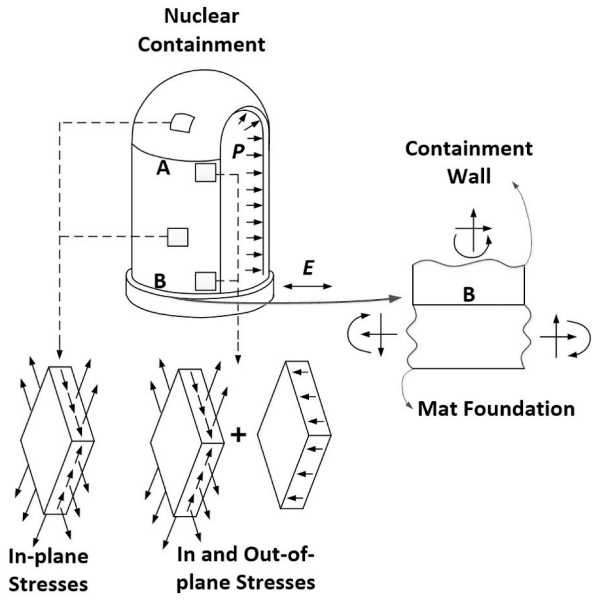

Fig. 4. In-plane and out-of-plane Stresses in a Nuclear Containment Wall

discontinuity through adjusted reinforcement ratios [11]. Shear reinforcement is critical in regions subjected to transverse or out-of-plane shear stresses.

A thorough understanding of SC elements under out-of-plane shear is vital because shear failure is inherently brittle in nature. Brittle shear failures are disastrous because it provides little or no warning before the structural capacity is reached. When configuring SC elements, it is crucial to secure their ductile behavior.

The shear resisting components of SC elements are similar to that of RC, consisting of the sandwiched concrete and embedded cross-ties. In RC structures, the longitudinal reinforcement is encased within the concrete, whereas in SC structures, the steel plates are positioned outside the concrete, exhibiting minimal or no bond with the concrete. A shear transfer mechanism is necessary to secure the steel plates to the concrete and transfer forces between them, ensuring force equilibrium. Shear connectors such as shear studs or cross-ties may be utilized to achieve coupling action between the composite structure.

Cross-ties (tie bars) are used exclusively in this research as shear connectors, serving dual roles: enabling composite action and enhancing shear capacity. Unlike prior studies that relied on shear studs or combined connectors [7,12], this approach simplifies design while acknowledging that full composite action may be uneconomical.

SC system stiffness depends on shear connector rigidity [9,13–15]. While rigid connectors could theoretically match the stiffness of doubly reinforced concrete, practical limitations cause bond-slip at the steel-concrete interface, degrading performance in terms of stiffness, strength, ductility and potentially altering the failure mode [13,14,16].

The out-of-plane behavior of SC walls relies on composite action between materials. Without shear connectors, the steel and concrete separate, rendering design code-based shear/flexural capacities invalid due to loss of assumed full composite action. The behavior of SC elements under out-of-plane shear (including shear strength, flexural strength, and interfacial shear (composite) strength) requires experimental validation. Existing design equations (e.g., ACI, UH method) conservatively predict shear resistance for RC/PSC beams [17–19], but their applicability to SC systems remains unverified. This study examines the behavior, failure mechanisms, and design standard applicability for SC systems using cross-ties under out-of-plane stresses.

2. Current specifications and code provisions

The following are the design codes and provisions available for predicting the flexural and shear capacities of SC elements. Most of these provisions were developed by assuming that there would not be a debonding failure between concrete and steel plate, and that the bond is perfect, similar to RC elements. In such a case, either the flexural or the shear capacity would govern the design. However, In SC structures with cross-ties only, the strength of the connection between the steel plate and the concrete is limited by the amount of cross-ties provided. Therefore, a third failure mode, called “Composite Capacity”, associated with debonding between two bound materials, may govern the design. The applicability of these design codes will be validated using the experimental database arranged for this study.

2.1. Flexural capacity

The flexural capacity of an SC wall subjected to out-of-plane forces can be determined using the following codes and specifications.

2.1.1. ACI 349M − 06 provisions

Based on ACI 349M-06 assumptions for doubly reinforced concrete beam, flexural capacity of SC elements can be estimated using adapted formulations. [20]. The assumptions include 1) a linear distribution of strain across the section, 2) maximum concrete compressive strain is limited to 0.003., 3) the strain in the steel plate is restricted to the yield strain in the extreme tension fiber of the steel plate, 4) the tensile contribution of concrete is not considered, and 5) an equivalent rectangular stress distribution for the concrete is considered with a reduction factor of 0.85 for the peak concrete compressive stress. Two additional assumptions are considered for SC elements.

1) To limit the compressive strain in the extreme compression fiber to the yield strain or the critical buckling strain of the compression steel plate. This is necessary not to violate the sectional force equilibrium conditions.
2) Steel plate and concrete are assumed to have full composite action, and the strain profile is linear and continuous over the entire section.

The derivation by Sener [7], which is based on the above assumptions, is used for calculating the flexural capacity of SC beams subjected to out-of-plane forces. The flexural capacity is given as

$$M_{n,ACI} = \left[A_s f_y (d - t_p) - \frac{1}{2} f_c' b_w c \left(\frac{c}{3} + \frac{t_s}{2} \right) \right] \tag{1}$$

$$c = 2t_p(n' - n), \text{where } c \geq 0 \tag{2}$$

where, c denotes the height of the triangular stress block in concrete above the neutral axis, A_s denotes the cross-sectional area of a single steel plate, t_s denotes the thickness of the steel plate, d denotes the depth, b_w denotes the section width, n denotes the modular ratio (E_s/E_c), and n' denotes the ratio of the steel plate yield stress to the concrete compressive strength (f_y/f_c').

2.1.2. JAEC-4618 technical code

The JAEC-4618 [21] is a technical standard for the seismic design of steel plate reinforced concrete structures, issued by the Japanese Electric Association Committee (JAEC). In the equation recommended by the technical code, the assumed lever arm, denotes the distance from the center of the steel plate on the tension side to the point where the resultant compressive force acts. This measurement, assumed to be $(7/8)d$, simplifies the calculation of flexural strength for SC elements under out-of-plane moments by defining the effective length of the lever arm within the structural element. The moment capacity of an SC beam according to theJAEC code is given as

$$M_{n,JAEC} = A_s f_y \frac{7}{8} d \tag{3}$$

2.1.3. AISC-N690 specifications

AISC-N690 [22] provides specifications for steel structures related to safety in nuclear facilities. This standard simplifies the calculation of the flexural strength of SC elements under out-of-plane moments by assuming a lever arm equal to $(0.9)d$. The formula given by the AISC-N690 code for calculating the moment capacity of an SC beam is as follows:

$$M_{n,AISC} = A_s f_y (0.9) d \tag{4}$$

2.1.4. KEPIC-SNG specifications

The KEPIC-SNG [23] is specifications for steel plate concrete structures related to safety for nuclear facilities, published by the Korea Electric Association. The equation is provided by the association to determine the flexural resistance capacity of SC elements under out-of-plane forces. The equation considers the contribution of stiffener elements and restricts the stresses in the compression steel plate to the critical buckling stress. The moment capacity of an SC element by KEPIC-SNG is given as

$$M_{n,SNG} = f_{y,\mathrm{cr}} A_s (d - t_s) + \left(f_y - f_{y,cr}\right) A_s \left(d - 1.5t_s - 0.5t_s \frac{f_y - f_{y,cr}}{0.85 f_c'}\right) + f_{y,rib} A_{rib} d_{rib} \tag{5}$$

$$f_{cr} = \left(1.5 - 0.0043 \frac{K_p S}{t_p} - 0.18 C_{cs}\right) f_y < f_y \tag{6}$$

where, $f_{y,rib}$ is the yield strength of the stiffener, A_{rib} is the area of the stiffener, and d_{rib} is the distance between the centroidal axes of the stiffener (ribs) on both steel plates.

2.2. Shear capacity

The shear capacity of an SC wall under out-of-plane forces can be determined using the following codes and specifications.

2.2.1. ACI 318–11 provisions

ACI 318–11 [24] has been developed for the design of Reinforced Concrete (RC) structures and applied in ACI 349 [25] to design of SC structures for seismic resilience. The nominal shear force (V_n) is calculated as the sum of the shear strength from concrete (V_C) and reinforcement (V_S).

$$V_{ACI} = V_c + V_s \tag{7}$$

$$V_c = \left(1.9\sqrt{f_c'} + 2500\rho_w \left(\frac{V_u d}{M_u}\right)\right) b_w d \le 3.5\sqrt{f_c'}\, b_w\, d. \tag{8}$$

$$Vs = A_v f_{yt} (d/s) \tag{9}$$

where, V_{ACI} is the nominal shear strength; V_c is the contribution of shear strength of concrete; V_s is the contribution of shear reinforcement; d is the effective depth of the section; f_c' is the concrete compressive strength in psi; V_u is the ultimate shear force; M_u is the ultimate bending moment; $M_u/(V_u d)$ is also the shear span to depth ratio (a/d), ρ_w is the longitudinal reinforcement ratio; b_w is the effective width in inches, $\rho_w = A_s/(bd)$, A_v is the area of shear reinforcements (cross-ties); f_{yt} is the yield strength of shear reinforcements (cross-ties); and s is the spacing of shear reinforcements (cross-ties).

Eq. (8) stipulates that the ratio $(V_u d)/M_u$ must not exceed 1.0, with V_c calculated as $\sqrt[2]{f_c'} b_w d$ for f_c' in psi, following ACI 318–11 guidelines. The basis of Eq. (8) in the guideline is a truss analogy, assuming a 45-degree failure crack, and it points to shear strength arising from shear reinforcement yielding, known as shear-tension failure. The ACI-ASCE Committee 326 warns that excessive web reinforcement may lead to shear-compression failure in concrete struts. Thus, to prevent concrete from crushing before transverse reinforcement yields, it is crucial to limit the shear contribution from shear reinforcement.

Minimum shear reinforcement is crucial to avoid abrupt shear failure. As per the ACI 318–11, the specifications for the minimum area and ratio of shear reinforcement are provided as follows:

$$A_{v,min} = 0.75\sqrt{f'_c}\,\frac{b_w S}{f_{yt}} \geq 50\frac{b_w S}{f_{yt}} \tag{10}$$

$$\rho_{t,ACI} = 0.75\frac{\sqrt{f'_c}}{f_{yt}} \geq 50\frac{1}{f_{yt}} \tag{11}$$

where, $A_{y,min}$ denotes the minimum area of shear reinforcement, $\rho_{t,ACI}$ denotes the shear reinforcement ratio, s denotes the spacing of cross-ties in a member of width b_w. f_{yt} is the yield strength of the rebars, and f'_c is the compressive strength of concrete at 28 days [24].

2.2.2. UH method (KUO et al., 2014)

The UH Method [19], developed by researchers at the University of Houston, offers a comprehensive shear design approach for both RC and PSC structures [26,27]. The shear strength of RC beams V_{UH} consists of the contribution of the concrete V_c and the shear reinforcement V_s. The formulas to determine the shear strength of RC beams are outlined in following equations. This method considers arch action by accounting for the ratio a/d, and the contribution of the concrete is based on the depth of the compression zone "c". The depth of the compression zone "c" can be determined using Eq. (14).

$$V_{UH} = V_c + V_s \tag{12}$$

$$V_C = 14\left(\frac{a}{d}\right)^{-0.7}\sqrt{f'_c}\,b_w\,c \leq 10\sqrt{f'_c}\,b_w\,c \tag{13}$$

$$\frac{c}{d} = \sqrt{2\,\rho_w\,n + (\rho_w\,n)^2} - \rho_w n \tag{14}$$

$$V_s = A_v\,f_{vy}\,(d/s - 1) \tag{15}$$

where, V_{UH} denotes the nominal shear strength; V_c denotes the shear contribution of concrete; V_s denotes the shear contribution from shear reinforcements; a/d denotes the ratio of shear span to effective depth; f'_c denotes the concrete compressive strength in psi; c denotes the depth of the un-cracked flexural compression zone; ρ_w denotes the longitudinal reinforcement ratio $\rho_w = A_s/(bd)$; $n = E_s/E_c$ modular ratio; E_s denotes the elastic modulus of steel reinforcement; E_c denotes the elastic modulus of concrete; A_v denotes the area of shear reinforcements (cross-ties); f_{yt} denotes the yield strength of shear reinforcements (cross-ties); and s denotes the spacing of shear reinforcements (cross-ties).

2.3. Composite capacity

There is no code provision for determining the composite capacity of SC elements subject to out-of-plane shear. Nonetheless, the interfacial shear capacity of an individual shear connector can be computed using specific codes and standards. The relevance of these formulas will be assessed through an experimental database.

2.3.1. AISC guidelines

The AISC code [28] provides equations to determine the interfacial shear strength of shear studs. The equations are provided for steel failure as well as concrete failure. The equations are given as

$$\textit{Steel Failure}: Q_u = A_s{*}f_{uv} \tag{16}$$

$$\textit{Concrete Failure}: Q_u = 0.5{*}A_s{*}\sqrt{f'_c{*}E_c} \tag{17}$$

where, Q_u denotes the interfacial shear strength of shear stud; A_s denotes the cross-sectional area of the shear connector; f_{uv} denotes the maximum tensile strength of the shear connector; f'_c denotes the concrete compressive strength; and E_c denotes the modulus of elasticity of concrete.

2.3.2. ACI 318-11 guidelines

The ACI code [24] offers formulas for computing the interfacial shear strength of shear studs, with specific equations for both steel failure and concrete failure. The formulas are presented as follow:

$$\textit{Steel Failure}: Q_u = 0.65{*}A_s{*}f_{uv} \tag{18}$$

$$\textit{Concrete Failure}: Q_u = 0.70{*}k_{cp}{*}\lambda\sqrt{f'_c} \tag{19}$$

where, Q_u denotes the interfacial shear strength of shear stud; A_s denotes the cross-sectional area of the shear connector; f_{uv} denotes the maximum tensile strength of the shear connector; f'_c denotes compressive strength of concrete; k_{cp} denotes coefficient for pry out

strength; λ donates modification factor reflecting the reduced mechanical properties of lightweight concrete, all relative to normal weight concrete of the same compressive strength.

2.3.3. IBC guidelines

The IBC code includes formulas to determine the interfacial shear strength of shear connectors, with specific equations for steel failure and concrete failure. The equations are specified as follow:

$$Steel\ Failure: Q_u = 0.8 * k_L * f_{uv} * \pi \frac{d^2}{4} \tag{20}$$

$$Concrete\ Failure: Q_u = 0.29 * d^2 * \left(f_c' * E_c\right)^{\frac{1}{2}} \tag{21}$$

$$k_L = (0.024t + 0.76)\frac{f_{yp}}{355}\ and\ k_L \leq 1 \tag{22}$$

where, Q_u denotes the interfacial shear strength of the shear connector; d denotes the diameter of the shear connector; f_{uv} denotes the maximum tensile strength of the shear connector; f_c' denotes the compressive strength of concrete; f_{yp} denotes the yield strength of steel plate; and t denotes the thickness of steel plate; k_L is an empirical factor related to the steel plate properties as defined in Eq. (22).

The interfacial shear strength equations in AISC, ACI318-11, and IBC differ due to variations in design philosophies, safety factors, failure mode considerations, and empirical adjustment. These differences reflect the distinct priorities of each code and the experimental databases underpinning them: AISC emphasizes steel reliability, ACI addresses concrete variability, and IBC integrates system-level effects.

3. Experimental database

Fig. 5 shows a scaled version of a strip from a nuclear containment wall that is part of the experimental database. The details of experimental program are published in separate journal papers by the authors [29,30]. The nuclear containment walls typically have a thickness ranging from 25 in. to 60 in. (508 mm–1524 mm) and steel plates have a thickness ranging from 0.25 in. to 1.5 in.(6.35 mm–38.1 mm). A 36″-thick (914.4 mm) overall nuclear containment wall with 0.42″ and 0.5625" (10.668 mm and 14.2875 mm) steel plate thicknesses was scaled by a factor of 4/9, such that large-scale testing could be performed on the PSC specimens within the experimental setup constraints of the laboratory. The scaled beam measures 15.0 feet (4572 mm) in length, 12.0 inches (305 mm) in width, and 16.0 inches (406 mm) in depth.

The experimental database for eight SC beams, along with their specifics, variables, ultimate load, and failure mechanism, are displayed in Table 1. The primary test parameters are the concrete strength, shear span-to-depth (a/d) ratio, slenderness ratio, and

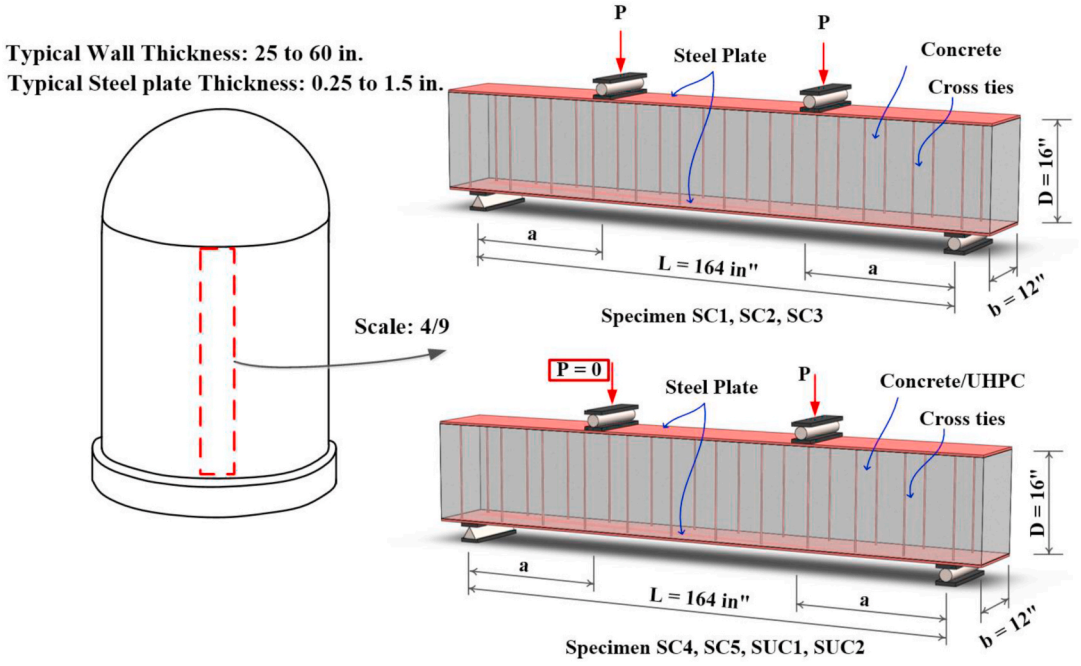

Fig. 5. A scaled strip of nuclear containment wall

cross-tie ratio ($\rho_{t,test}$). When the shear span-to-depth (a/d) ratio is 2.5, reinforced concrete (RC) elements subjected to a concentrated load display minimum shear strength [31]. Tests conducted on Prestressed Concrete (PSC) beams caught this phenomena [26]. A minimal amount of shear reinforcement for the PSC part was suggested based on the test findings. The suggested sum was twice as much as what the ACI 349 guidelines said for an a/d between 2.0 and 4.0 [26,27]. Consequently, three a/d values—1.5, 2.5, and 5.2—were determined, and the range of $\rho_{t,test}$ was varied from 0.102 % to 0.323 %. The distance between the center line of the actuator and the support, as depicted in Fig. 5, is known as the shear span a. Similarly, the depth d is the distance between the center line of the bottom steel plate and the extreme top fiber. ACI 349 provisions equation (11) was used in the design of the cross-ties in Specimen SC1 and SUC1 North to confirm that the minimum shear reinforcement requirements [25] applied to SC and S-UHPC beams.

3.1. Material properties

Based on the intended shear reinforcement ratio, the diameter of the rebars and the cross-tie spacing (s) were computed. Shear reinforcement was provided by deformed No. 2 reinforcing bars, while top and bottom steel plates for SC1 through SC6 were made of 3/16-inch (4.76 mm) high-strength low-alloy structural steel (ASTM A572-50 [32]).The top and bottom steel plates for specimen SUC1 and SUC2 were made of 0.25-inch (6.35 mm) grade 70 high strength steel that complied with ASTM/ASME SA 516. No. 3 rebars were utilized as the shear reinforcement. A total of 3 coupon tests and 3 rebar tension tests were performed to capture the yield strength and tensile strength of the steel plate and rebar and the average values were reported in Table 2, respectively.

Specimens SC1 through SC6 were cast using normal strength concrete, which has a strength range of 5–8 ksi (34.474 MPa–55.158 MPa). Specimens SUC1 and SUC2 were made of Ultra-High Performance Concrete (UHPC), which has a compressive strength of 22 ksi (151.7 MPa).

The specimen naming system follows a clear and consistent format to describe key experimental parameters. The prefix "SC" denotes a Steel Plate-Concrete (SC) composite specimen, while "SUC" indicates a Steel Plate-UHPC (Ultra-High-Performance Concrete) specimen. The numerical value immediately following these prefixes serves as a unique specimen identifier (e.g., SC1, SUC2). The first hyphenated number specifies the critical shear span-to-depth ratio (a/d). Subsequent notations include "S" followed by a number representing the cross-tie spacing in inches (converted to millimeters in parentheses where applicable), and a final "N" or "S" indicating whether loading was applied on the north or south side of the specimen. For example, specimen SC1-2.5-S8-N describes a standard steel plate-concrete specimen (SC1) with a shear span-to-depth ratio of 2.5, cross-ties spaced at 8 inches (203.2 mm), and north-side loading application.

3.2. Loading protocol and test setup

The specimens underwent vertical loading using north and/or south actuators, each with a capacity of 600 kips (2670 kN), as shown in Fig. 6(a). The loading process, controlled by the MTS Flex system, included several steps, and managed both loads and displacements of the actuators. Each loading step was conducted at a constant rate of 0.10 inch (2.54 mm) every 15 minutes. During these steps, loading could be paused and resumed to inspect and document any cracks. Each test spanned three to five hours. The

Table 1
Summary of experimental parameters and failure modes of SC elements under for out-of-plane loading.

No.	Specimen Identifier	f_c' (MPa)	$\frac{a}{d}$	ρ %	d (mm)	s (mm)	$\rho_{t,test}$ %	P_{ult} (kN)	Test Failure Mode
Conventional Concrete - f_c' (34.5–55.2) MPa									
Steel plate Thickness - t_s (4.76)mm, f_y (441.26 MPa), f_u (537.79 MPa) d_b (6.35 mm, #2 rebar), f_y (419.2 MPa), f_u (613.63 MPa)									
1	SC1-2.5-S8-N	56.05	2.5	2.36	404.11	203.2	0.102	121.88	Interfacial Shear
2	SC1-2.5-S8-S	56.05	2.5	2.36	404.11	203.2	0.102	116.09	Interfacial Shear
3	SC2-2.5-S7-S	39.98	2.5	2.36	404.11	177.8	0.117	120.10	Interfacial Shear
4	SC3-2.5-S6-N	40.13	2.5	2.36	404.11	152.4	0.137	141.01	Interfacial Shear
5	SC3-2.5-S6-S	40.13	2.5	2.36	404.11	152.4	0.137	154.79	Interfacial Shear
6	SC4-2.5-S5-N	50.81	2.5	2.36	404.11	127	0.164	189.93	Interfacial Shear
7	SC4-2.5-S4-S	50.81	2.5	2.36	404.11	101.6	0.205	236.20	Flexural Tension
8	SC5-1.5-S6-S	55.16	1.5	2.36	404.11	152.4	0.137	121.88	Shear Tension
9	SC5-1.5-S5-N	55.16	1.5	2.36	404.11	127	0.164	116.09	Shear Tension
10	SC6-5.2-S6	55.16	5.2	2.36	404.11	152.4	0.137	120.10	Flexural Tension
Ultra-high Performance Concrete - f_c' (~151.68 MPa)									
Steel plate Thickness - t_s (6.35 mm), f_y (510.21 MPa), f_u (606.39 MPa) d_b (9.53 mm, #3 rebar), f_y (458.5 MPa), f_u (602.60 MPa)									
11	SUC1-2.5-10-S	154.03	2.5	3.14	403.35	254	0.184	220.19	Interfacial Shear
12	SUC1-2.5-8-N	154.03	2.5	3.14	403.35	203.2	0.231	206.84	Interfacial Shear
13	SUC2-2.5-6.75-S	153.89	2.5	3.14	403.35	171.45	0.277	346.07	Interfacial Shear
14	SUC2-2.5–5.75-N	153.89	2.5	3.14	403.35	146.05	0.323	382.10	Flexural Tension

Note.
[1]. P_{ult} is the highest load P achieved during the experimental procedure as per the loading protocol described in Fig. 5.
[2]. f_c' is the compressive strength of the concrete determined by testing three 4″x8″ cylinders on the day of testing the specimen.

Table 2
Mechanical properties of the materials.

Material	*Diameter/Thickness(mm)*	f_y *(MPa)*	f_u *(MPa)*
No. 2 Rebars	6.35	419.20	613.63
Grade 50 Steel plate	4.76	441.26	537.79
No.3 Rebars	9.53	458.50	602.60
Grade 70 Steel plate	6.35	510.21	606.39

Notes: f_y = Yield stress, f_u = Maximum tensile stress.

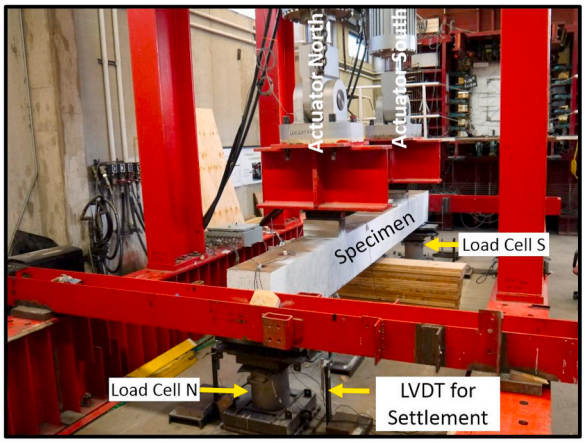

a) Loading arrangement

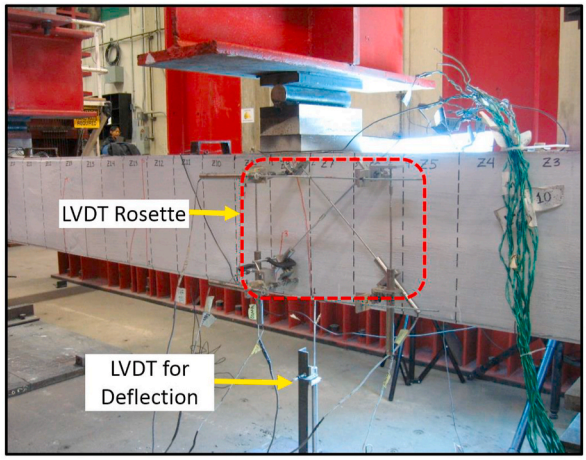

b) LVDT Setup

Fig. 6. Test setup of the specimen

displacement control feature played a crucial role in observing the post-peak behavior of the SC beams.

Specimens SC1 and SC3 underwent simultaneous loading at both their north and south ends. In contrast, an issue with the control system during the symmetrical loading of SC2 led to an early failure at the north end, leaving the south end unaffected and not subjected to load, hence SC2 was loaded solely at the south end afterward. For specimens SC4, SC5, SUC1, and SUC2, each end was tested sequentially, shifting support to the nearest intact section after a failure occurred, as seen with SC4 south and SC5 north ends. Specimen SC6 uniquely experienced loading at its central span via a single actuator.

4. General behavior and modes of failure

The fourteen experiments conducted on eight simply supported SC beams make up the experimental database. Specimen SC1 and SUC1-South were designed as per the minimum shear reinforcement provision of the ACI code. Specimens SC2, SC3, SC4, SUC1-North, and SUC2 were designed with an increasing amount of cross-tie ratio. The purpose of specimens SC5 and SC6 was to examine the impact of the a/d ratio.

A common observation in the specimens was the formation of an inclined crack within the shear span area, which subsequently initiated bond-slip at the interface between the concrete and the bottom steel plate. The failure mode of the beam—whether from debonding, shear tension, or flexural tension—varied based on the quantity of cross-ties used. Notably, none of the tests exhibited compression shear or compression flexure failures.

In specimens with a low amount of cross-ties, debonding would significantly develop at earlier loading stages. The cross-ties would not yield, and due to large cracking, the beams would lose its load bearing capacity and fail due to debonding in a sudden and brittle manner.

In specimens with a higher amount of cross-ties, there could be three possible failure modes.

1) The cross-ties at the interface would yield, providing some ductility before ultimately failing. This failure mode is categorized as debonding.
2) The cross-ties possessed sufficient composite capacity to enable those at the center of the beam cross-section to yield under high shear stresses, leading to a failure mode characterized by shear tension.
3) The cross-ties would have enough composite capacity and shear capacity to allow the steel plate yield resulting in flexural tension failure mode.

As an example, the failure pattern of Specimen SUC2-2.5–5.75-N is shown in Fig. 7. After the initiation of the inclined crack, bond-slip between the steel plate and concrete began to develop. However, the composite capacity and shear capacity provided by the cross-ties in this specimen was sufficient to allow the steel plate to yield, resulting in flexural tension failure.

5. Applicability of design codes

Using ACI and UH equations, the shear capacity for all test specimens was determined and compared with the experimental results in Table 3.

It can be observed from the tabulated results that ACI and UH equations could not predict the shear capacity of SC/SUC beams except for specimen SC5-1.5-S6-S and SC5-1.5-S5-N. For the ACI and UH equations to be applicable, the composite capacity of the SC system needs to be greater than the shear capacity. For specimen SC5-1.5-S6-S and SC5-1.5-S5-N, the composite capacity was sufficient to reach the desired failure mode, which was the shear failure mode.

The flexural capacity for all test specimens was determined through the transformed section method, incorporating the cracked moment of inertia and employing methods from ACI, JAEC, AISC, and the Korean standards. The results for each method are tabulated and analyzed alongside the experimental data in Table 4.

Initially, most of the specimens were designed to predominantly exhibit shear failure mode. Specimens SC4-2.5-S4-S, SC6-5.2-S6 and SUC2-2.5–5.75-N failed in flexural tension. The composite action and shear capacity provided by the cross-ties in these specimens were larger than the flexural capacity of the section. Therefore, the bottom steel plate in these specimens yielded before the composite action capacity or the shear capacity was reached. The equations provided by all of the methods could calculate an SC beam's flexural

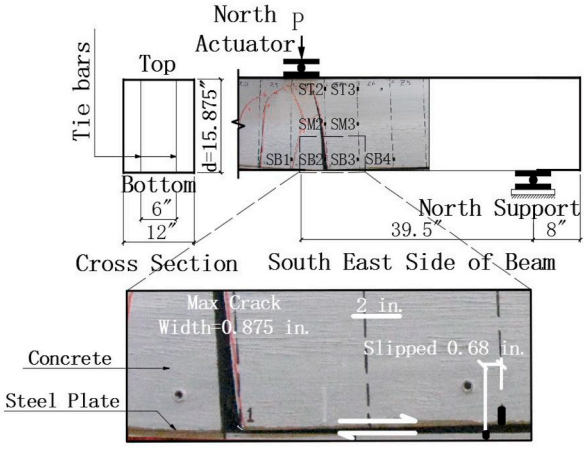

Fig. 7. Failure pattern of SUC2-2.5–5.75-N

Table 3
Shear capacity by ACI and UH and comparison with test results (Unit:kN).

No.	Specimen Identifier	V_{test} (kN)	Shear						Comparison	
			ACI (kN)			UH (kN)			$\frac{V_{test}}{V_{ACI}}$	$\frac{V_{test}}{V_{UH}}$
			V_s (Eq. (8))	V_c (Eq. (9))	V_{ACI} (Eq. (7))	V_s (Eq. (13))	V_c (Eq. (15))	V_{UH} (Eq. (12))		
1	SC1-2.5-S8-N	121.88	52.93	157.47	210.40	26.24	173.48	199.73	0.58	0.61
2	SC1-2.5-S8-S	116.10	52.93	157.47	210.40	26.24	173.48	199.73	0.55	0.58
3	SC2-2.5-S7-S	119.66	60.50	134.34	194.83	33.81	156.58	190.83	0.62	0.63
4	SC3-2.5-S6-N	144.57	70.28	134.78	205.06	44.04	157.02	201.06	0.70	0.72
5	SC3-2.5-S6-S	156.13	70.28	134.78	205.06	44.04	157.02	201.06	0.76	0.78
6	SC4-2.5-S5-N	189.94	84.52	150.35	234.87	58.27	168.14	226.41	0.81	0.84
7	SC4-2.5-S4-S	235.76	105.42	150.35	255.77	79.18	168.14	247.77	0.92	0.95
8	SC5-1.5-S6-S	248.66	70.28	162.80	233.09	44.04	246.43	290.47	1.07	0.86
9	SC5-1.5-S5-N	287.80	84.52	162.80	247.32	58.27	246.43	304.70	1.16	0.95
10	SC6-5.2-S6	127.7	70.3	151.2	221.5	44.04	103.2	147.2	0.58	0.87
11	SUC1-2.5-10-S	220.19	95.19	257.11	352.30	35.14	262.00	297.14	0.62	0.74
12	SUC1-2.5-8-N	206.84	118.77	257.11	375.87	59.16	262.00	321.16	0.55	0.64
13	SUC2-2.5-6.75-S	346.07	152.57	257.11	409.68	80.96	262.45	343.40	0.84	1.01
14	SUC2-2.5–5.75-N	382.10	178.82	257.11	435.93	105.42	262.45	367.87	0.88	1.04
	Average								0.76	0.80
	Standard Deviation								0.20	0.15
	COV								0.26	0.19

Note.
1. $\boldsymbol{V_{test}}$ is the highest load $\boldsymbol{P}$ achieved during the experimental procedure as per the loading protocol described in Fig. 5.

Table 4
Flexural Capacity Calculations and Comparison(Unit: kN.m).

Specimen Identifier	M_T (kNm)	Flexure (kNm)					Comparison				
		$M_{Tr.}$	M_{ACI}	$M_{J.}$	$M_{A.}$	$M_{K.}$	$\frac{M_T}{M_{Tr.}}$	$\frac{M_T}{M_{ACI}}$	$\frac{M_T}{M_{J.}}$	$\frac{M_T}{M_{A.}}$	$\frac{M_T}{M_{K.}}$
SC1-2.5-S8-N	123.94	270.60	259.41	231.39	237.95	257.49	0.46	0.48	0.54	0.52	0.48
SC1-2.5-S8-S	117.96	270.60	259.41	231.39	237.95	257.49	0.44	0.45	0.51	0.50	0.46
SC2-2.5-S7-S	121.80	270.60	256.93	231.39	237.95	258.51	0.45	0.47	0.53	0.51	0.47
SC3-2.5-S6-N	146.65	270.60	256.93	231.39	237.95	259.98	0.54	0.57	0.63	0.62	0.56
SC3-2.5-S6-S	158.63	270.60	256.93	231.39	237.95	259.98	0.59	0.62	0.69	0.67	0.61
SC4-2.5-S5-N	193.09	270.60	258.85	231.39	237.95	261.00	0.71	0.75	0.83	0.81	0.74
SC4-2.5-S4-S	239.42	270.60	258.85	231.39	237.95	261.00	0.88	0.93	1.03	1.01	0.92
SC5-1.5-S6-S	151.63	270.60	259.30	231.39	237.95	260.20	0.56	0.58	0.66	0.64	0.58
SC5-1.5-S5-N	175.58	270.60	259.30	231.39	237.95	261.00	0.65	0.68	0.76	0.74	0.67
SC6-5.2-S6	269.58	270.60	259.30	231.39	237.95	260.20	1.00	1.04	1.17	1.13	1.04
SUC1-2.5-10-S	223.48	399.18	347.20	351.16	361.21	343.81	0.56	0.64	0.64	0.62	0.65
SUC1-2.5-8-N	210.27	399.18	347.20	351.16	361.21	345.62	0.53	0.61	0.60	0.58	0.61
SUC2-2.5-6.75-S	351.50	399.18	347.20	351.16	361.21	346.52	0.88	1.01	1.00	0.97	1.01
SUC2-2.5–5.75-N	388.10	399.18	347.20	351.16	361.21	347.09	0.97	1.12	1.11	1.07	1.12
Average							0.66	0.71	0.76	0.74	0.71
Standard Deviation							0.20	0.22	0.23	0.22	0.22
COV							0.30	0.31	0.30	0.30	0.31

Notes: M_{Tr} = Transformed cracked moment capacity, M_{ACI} = Moment capacity based on ACI; M_J = Moment capacity based on JAEC. M_A = Moment capacity based on ASCE. M_K = Moment capacity based on Korean method.

capacity accurately, given that the composite action capacity provided is sufficient to achieve the desired flexural failure mode.

6. Composite capacity

The shear capacity V_n for most of the experimental test results was lower than the shear capacities calculated from the ACI and UH equations. Furthermore, the moment capacity M_n calculated from codes and guidelines did not match with the experimental moment capacities of most of the specimens. This is a result of insufficient composite action at the steel plate and concrete interaction to keep the forces in equilibrium. The capacity of the shear connectors to resist interfacial shear force, calculated using AISC, ACI, and IBC design codes and guidelines, was found to be conservatively estimated and did not accurately predict the actual capacity.

The three codes do not account for friction at the interface due to normal forces. Accounting for friction using a coefficient of 0.7 resulted in an accurate prediction of the composite action capacity [33]. An equation is derived to predict the composite capacity of SC elements by considering the frictional forces combined with the contribution of cross-ties calculated from AISC specifications. A free

body diagram, as shown in Fig. 8, illustrates the forces on the beam between the point where the load is applied and the end of the beam. From this diagram, the following expressions can be formulated.

By equilibrium:

$$T_{max} = \int_0^{(a+z)} V_{Interface} dx \tag{23}$$

$$T_{max} = \mu^* V_{max} + \frac{(a+z)}{S}^* A_V^* f_{uv} \tag{24}$$

$$f_y = \frac{T_{max}}{A_s} = \frac{\mu^* V_{max}}{A_s} + \frac{(a+z)}{S}^* \frac{A_V}{A_s}^* f_{uv} \tag{25}$$

Considering:

$$V_{max} = \frac{M_{max}}{a} \tag{26}$$

$$M_{max} = A_s^* f_y^* jd \tag{27}$$

where, $jd = 0.875^* D$ based on JAEC specifications, the equation for f_{yslip} for design purposes is derived as follows

$$f_y = \frac{\mu^* M_{max}}{a^* A_s} + \frac{(a+z)}{S}^* \frac{A_V}{A_s}^* f_{uv} \tag{28}$$

$$f_y = \frac{\mu^* jd^* A_s^* f_y}{a^* A_s} + \frac{(a+z)}{S}^* \frac{A_V}{A_s}^* f_{uv} \tag{29}$$

$$f_{yslip} = \frac{(a+z)}{S}^* \frac{A_V}{A_s}^* \frac{f_{uv}}{\left(1 - \mu^* \left(\frac{a}{jd}\right)^{-1}\right)} \leq f_y \tag{30}$$

The value of $jd = 0.875^* D$ based on JAEC specifications was selected as the most predictive for determining the moment capacity of composite SC sections. The comparison between the steel plate stresses was defined by the new model, and test results are shown in Table 5. The equation starts to diverge for smaller a/d ratios due to the arch action becoming more predominant. Therefore, the applicability of the proposed equation is limited to a/d ratios of greater than 1.5.

The composite capacity is also the maximum tensile force in the steel plate $T_{\max}$, given as

$$T_{max} = \mu^* V_{max} + n^* A_V^* f_{uv} \tag{31}$$

where, μ is the friction coefficient of the interface, V is the normal force in the shear span (Shear force), n is the number of cross-ties in the shear span, A_v is the area of a single cross-tie and f_{uv} is the ultimate tensile capacity of the cross-tie.

The composite capacity or the maximum steel plate tensile force is calculated for each specimen and subsequently converted into equivalent shear force. The equivalent composite action shear force (C_n) could be determined using equation (33). The moment capacity equation by JAEC is considered for calculating the equivalent composite action shear force.

$$M_{n,JAEC} = T_{max} \frac{7}{8} d \tag{32}$$

$$C_n = V_{max} = \frac{M_{max}}{a} = \frac{7}{8} \frac{T_{max}}{(a/d)} \tag{33}$$

The experimental results and code comparisons for composite action are tabulated in Table 6. In Table 6, T_{Steel} and $T_{Concrete}$ are the steel and concrete capacities calculated using equations provided in section 2.3. Furthermore, T_{AISC}, T_{ACI}, T_{IBC} is the minimum of T_{steel} or $T_{concrete}$ for the respective code. Table 6 comparison shows that the interfacial shear capacity equations by AISC, ACI and IBC are grossly conservative. In comparison, the interfacial shear capacity equation developed in this paper and compared to test results in Table 5 is accurate in predicting the interfacial shear capacity of the steel plate concrete beams.

7. Conclusions

- Cross-ties, known as tie bars, effectively transfer shear between the steel plate and concrete. They not only facilitate composite action but also serve as shear reinforcement, enhancing the shear carrying capacity of the SC beam.
- The initial chemical bond between the two materials was observed to fail at the early stages of loading. The subsequent bond was maintained by the cross-ties and the friction resulting from normal forces.

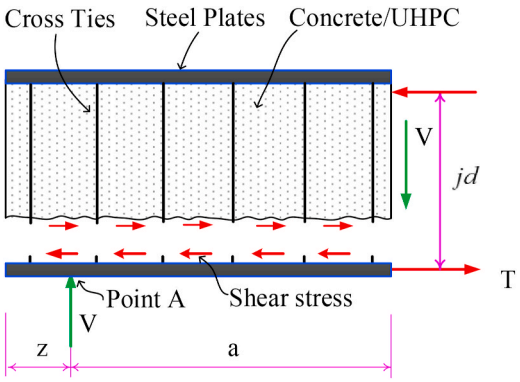

Fig. 8. Free body diagram of SC/S-UHPC beam

Table 5
Comparison of the steel plate design model and experimental results.

Specimen Identifier	$f_{y,Test}$ (kN)	$f_{y,Model}$ (kN)	$\frac{f_{y,Test}}{f_{y,Model}}$	$M_{n,Test}$ (kNm)	$M_{n,Model}$ (kNm)	$\frac{M_{n,Test}}{M_{n,Model}}$
SC1-2.5-S8-N	215.12	219.25	0.98	123.83	113.21	1.09
SC1-2.5-S8-S	213.74	219.25	0.97	117.96	113.21	1.04
SC2-2.5-S7-S	213.74	250.28	0.85	121.68	129.37	0.94
SC3-2.5-S6-N	302.68	292.34	1.04	146.65	150.95	0.97
SC3-2.5-S6-S	328.88	292.34	1.13	158.63	150.95	1.05
SC4-2.5-S5-N	359.91	350.94	1.03	192.98	181.23	1.07
SC4-2.5-S4-S	439.89	438.51	1.00	239.42	226.42	1.06
SC5-1.5-S6-S	339.91	248.90	1.37	151.63	128.46	1.18
SC5-1.5-S5-N	357.15	298.54	1.20	175.47	154.11	1.14
SC6-5.2-S6	441.26	441.26	1.00	269.58	231.39	1.17
SUC1-2.5-10-S	335.77	295.79	1.13	223.48	203.82	1.10
SUC1-2.5-8-N	319.23	369.56	0.86	210.27	254.78	0.83
SUC2-2.5-6.75-S	430.92	438.51	0.98	351.50	302.01	1.16
SUC2-2.5–5.75-N	523.31	521.24	1.00	388.10	308.45	1.26
Average			1.04			1.08
Standard Deviation			0.13			0.11
COV			0.13			0.10

Table 6
Composite Capacity and Comparisons (Unit: kN).

Specimen Identifier	T_{test}	Composite Capacity									Comparison		
		AISC			ACI			IBC					
		T_{Steel}	$T_{Concrete}$	T_{AISC}	T_{Steel}	$T_{Concrete}$	T_{ACI}	T_{Steel}	$T_{Concrete}$	T_{IBC}	$\frac{T_{Test}}{T_{AISC}}$	$\frac{T_{Test}}{T_{ACI}}$	$\frac{T_{Test}}{T_{IBC}}$
SC1-2.5-S8-N	347.0	231.3	266.9	231.3	151.2	422.6	151.2	106.8	111.2	106.8	1.50	2.29	3.25
SC1-2.5-S8-S	333.6	231.3	266.9	231.3	151.2	422.6	151.2	106.8	111.2	106.8	1.44	2.21	3.13
SC2-2.5-S7-S	342.5	271.3	240.2	271.3	177.9	355.9	177.9	124.6	102.3	102.3	1.43	1.93	3.35
SC3-2.5-S6-N	413.7	311.4	275.8	275.8	200.2	355.9	200.2	137.9	115.7	115.7	1.50	2.07	3.58
SC3-2.5-S6-S	444.8	311.4	275.8	275.8	200.2	355.9	200.2	137.9	115.7	115.7	1.61	2.22	3.85
SC4-2.5-S5-N	542.7	387.0	413.7	387.0	253.5	404.8	253.5	173.5	173.5	129.0	1.40	2.14	3.13
SC4-2.5-S4-S	671.7	467.1	498.2	467.1	302.5	404.8	302.5	209.1	204.6	204.6	1.44	2.22	3.28
SC5-1.5-S6-S	427.0	231.3	262.4	231.3	151.2	418.1	151.2	106.8	111.2	106.8	1.85	2.82	4.00
SC5-1.5-S5-N	493.8	271.3	306.9	271.3	177.9	418.1	177.9	124.6	129.0	124.6	1.82	2.78	3.96
SC6-5.2-S6	756.2	582.7	658.3	582.7	378.1	418.1	378.1	262.4	271.3	262.4	1.30	2.00	2.88
SUC1-2.5-10-S	627.2	471.5	1067.6	471.5	284.7	702.8	284.7	155.7	351.4	155.7	1.33	2.20	4.03
SUC1-2.5-8-N	591.6	564.9	1281.1	564.9	342.5	702.8	342.5	186.8	422.6	186.8	1.05	1.73	3.17
SUC2-2.5-6.75-S	987.5	751.7	1708.1	751.7	453.7	702.8	453.7	249.1	560.5	249.1	1.31	2.18	3.96
SUC2-2.5–5.75-N	1089.8	845.2	1921.6	845.2	511.5	702.8	511.5	280.2	631.6	280.2	1.29	2.13	3.89
Average											1.45	2.21	3.53
Standard Deviation											0.21	0.29	0.41
COV											0.15	0.13	0.12

- Sudden brittle failure occurred when the number of cross-ties provided met only the minimum shear reinforcement requirements of ACI 318–11. The composite capacity between the two materials was insufficient to achieve the shear capacity dictated by the minimum reinforcement provided.
- A targeted failure mechanism, such as flexure or shear, can only be achieved if sufficient composite capacity is provided. Without this, "debonding", the failure mechanism associated with composite action, would govern.
- The ACI code and UH method proved accurate in estimating the shear capacity of beams, assuming the contribution of cross-ties to composite action and shear is well understood.
- Equation derived based on AISC provisions predicted the provided composite action accurately.
- A steel plate model is proposed for design calculations. The model is derived based on AISC specifications. The derived model takes into account all the physical parameters that govern the maximum stress development in the steel plate of an SC beam under out-of-plane forces.
- Specimens SC5 North and South failed in the shear tension failure mode. The provided composite action was sufficient for the beam to reach the shear capacity. The equations provided by ACI code predicted the shear capacity accurately.
- Specimen SC4 South, SC6, and Specimen SUC2 North exhibited a flexural tension failure mode due to the yielding of the bottom steel plate. The composite action from the cross-ties in these beams was sufficient to enable the specimens to reach this mode of failure. In essence, the composite action capacity and shear capacity exceeded the flexural capacity of the beam. The formulas from ACI, JAEC, AISC, and KEPIC-SNG accurately predicted the flexural capacity.

CRediT authorship contribution statement

Jamshaid Sawab: Writing – original draft, Validation, Project administration, Methodology, Data curation. **Avinash Gautam:** Resources, Project administration. **Peng Liang:** Resources, Investigation. **Jiaji Wang:** Writing – review & editing, Supervision, Data curation, Conceptualization. **Y.L. Mo:** Writing – review & editing, Supervision, Funding acquisition.

Declaration of competing interest

The authors declare that they have no known competing financial interests or personal relationships that could have appeared to influence the work reported in this paper.

Acknowledgements

The research described in this paper is financially supported by U.S. Department of Energy NEUP program under Project No. CFP-13-5282.

Data availability

Data will be made available on request.

References

[1] J. Tolloczko, Bi-Steel in tall buildings, New Steel Construct. 9 (6) (2001) 34–35.
[2] W. Zhang, Study on mechanical behavior and design of composite segment for shield tunnel, in: Graduate School of Science and Engineering, WASEDA University, Tokyo, 2009.
[3] J.-B. Yan, et al., Experimental and analytical study on ultimate strength behavior of steel–concrete–steel sandwich composite beam structures, Mater. Struct. (2014) 1–22.
[4] T.L. Schulz, Westinghouse AP1000 advanced passive plant, Nucl. Eng. Des. 236 (14–16) (2006) 1547–1557.
[5] J. Sawab, Composite Steel Plate Concrete (SC) Structures: Theory and Experiment, University of Houston, 2019.
[6] M. Takeuchi, et al., Study on a concrete filled structure for nuclear power plants, Nucl. Eng. Des. 179 (2) (1998) 209–223.
[7] K.C. Sener, Out-of-plane Behavior and Design of Steel-Plate Composite (SC) Walls for Safety-Related Nuclear Facilities, Purdue University, 2014.
[8] T.T.C. Hsu, Y.L. Mo, Unified Theory of Concrete Structures, John Wiley & Sons, 2010.
[9] M. Xie, N. Foundoukos, J. Chapman, Static tests on steel–concrete–steel sandwich beams, J. Constr. Steel Res. 63 (6) (2007) 735–750.
[10] N. Subedi, Double skin steel/concrete composite beam elements: experimental testing, Struct. Eng. 81 (21) (2003) 30–35.
[11] J.J. Ucciferro, Effects of permissible shear stress on the design and construction of reinforced concrete containments, Nucl. Eng. Des. 69 (2) (1982) 195–203.
[12] K.C. Sener, A.H. Varma, D. Ayhan, Steel-plate composite (SC) walls: out-of-plane flexural behavior, database, and design, J. Constr. Steel Res. 108 (2015) 46–59.
[13] H. Wright, T. Oduyemi, Partial interaction analysis of double skin composite beams, J. Constr. Steel Res. 19 (4) (1991) 253–283.
[14] N.R. Coyle, Development of Fully Composite Steel-Concrete-Steel Beam Elements, University of Dundee, 2001.
[15] T. Roberts, D. Edwards, R. Narayanan, Testing and analysis of steel-concrete-steel sandwich beams, J. Constr. Steel Res. 38 (3) (1996) 257–279.
[16] N. Foundoukos, Behaviour and Design of Steel-Concrete-Steel Sandwich Construction, University of London, Imperial College of Science, Technology and Medicine, London, 2005.
[17] A. Laskar, Shear Behavior and Design of Prestressed Concrete Members, University of Houston, 2009.
[18] Wu Wei Kuo, T.T.C.H. and H. Shyh Jiann, Shear strength of reinforced concrete beams. Structural Journal. 111(4).
[19] W.W. Kuo, T.T.C. Hsu, S.J. Hwang, Shear strength of reinforced concrete beams, ACI Struct. J. 111 (4) (2014).
[20] ACI-349, Code Requirements for Nuclear Safety-Related Concrete Structures:(ACI 349-06) and Commentary, an ACI Standard, American Concrete Institute, 2006.
[21] JAEC, Technical code for seismic design of Steel Plate reinforced concrete structures: buildings and structures, in: Translated from Japanese by Obayashi Company and Westinghouse Electric Company, 2009. Tokyo, Japan.
[22] AISC-N690-12-Supplement-No.1, Specification for Safety-Related Steel Plate Concrete Structures for Nuclear Facilities, AISC, Chicago, IL, 2015.

[23] KEPIC-SNG, Specification for Safety-Related STeel Plate Concrete Structures for Nuclear Facilities, Board of KEPIC Policy, Structural Committee, Korea Electric Association, Tokyo, Japan, 2010.
[24] ACI-318, Building Code Requirements for Structural Concrete (ACI 318-11) and Commentary, American Concrete Institute, 2011.
[25] ACI Committee 349, Code Requirements for Nuclear Safety-Related Concrete Structures: (ACI 349-06) and Commentary, American Concrete Institute, Farmington Hills, Michigan, 2006.
[26] Laskar, A., T.T.C. Hsu, and Y.L. Mo, Shear strengths of prestressed concrete beams Part 1: experiments and shear design equations. Structural Journal. 107(3).
[27] Hsu, T.T.C., A. Laskar, and Y.L. Mo, Shear strengths of prestressed concrete beams Part 2: comparisons with ACI and AASHTO provisions. Structural Journal. 107(3).
[28] A. Committee, Specification for Structural Steel Buildings (ANSI/AISC 360-10), American Institute of Steel Construction, Chicago-Illinois, 2010.
[29] J. Sawab, et al., Structural integrity of steel plate ultra high-performance concrete modules, Journal of Structural Integrity and Maintenance 1 (3) (2016) 95–106.
[30] F. Qin, et al., Minimum shear reinforcement ratio of steel plate concrete beams, Mater. Struct. 49 (9) (2016) 3927–3944.
[31] G. Kani, The riddle of shear failure and its solution, ACI Journal 61 (4) (1964) 441–467.
[32] ASTM Standard A572, Standard Specification for High-Strength Low-Alloy Columbium-Vanadium Structural Steel (A572/A572M-13a), ASTM, West Conshohocken, Pennsylvania, 2014.
[33] Jason Mccormick, et al., Investigation of the sliding behavior between steel and mortar for seismic applications in structures, Earthq. Eng. Struct. Dynam. 38 (12) (2009) 1401–1419.